

# **Smart Manufacturing and Material Processing** (SMMP)

DOI: http://doi.org/10.26480/smmp.01.2023.96.101



#### RESEARCH ARTICLE



# DESIGN AND EVALUATION OF AUXETIC STRUCTURES AS DISPLACEMENT SENSOR

Hao Tian, Pengju Li, Qingguo Wen, Zhengkai Zhang\*

School of Mechanical and Electrical Engineering, Xi'an University of Architecture and Technology, Xi'an China. \*Corresponding Author Email: woodncy@163.com

This is an open access article distributed under the Creative Commons Attribution License CC BY 4.0, which permits unrestricted use, distribution, and reproduction in any medium, provided the original work is properly cited.

#### **ARTICLE DETAILS**

#### Article History:

Received 05 January 2024 Revised 08 February 2024 Accepted 11 March 2024 Available online 14 March 2024

#### **ABSTRACT**

In the field of engineering measurement, the displacement sensor is a widely used tool. In this study, a novel method has been developed for measuring displacement. The newly introduced approach aims to address the demand for improved sensitivity, accuracy, and efficiency in displacement measurements, thereby contributing to advancements in various engineering applications and providing valuable insights for future sensor development. The proposed method involves the conversion of stress deformation-induced position changes in auxetic structures into output current changes, providing acceptable measurement accuracy and reliable means of measuring displacement. To evaluate the efficacy of proposed method, three different structures are utilized for analysis and experimental testing in this study, and their performance is comparatively evaluated. The discoveries in this study will present fresh possibilities for employing auxetic materials in the domain of measurement. 3D printing technology is employed for the fabrication of the auxetic structures, rather than conventional subtractive manufacturing methods. 3D printing technology has completely revolutionized various industries, and in the field of measurement, its potential remains largely untapped. By exploring innovative applications, we can expand its utility, simplify the complexity associated with sensor manufacturing, and achieve significant cost reductions. This article delves into the exciting possibilities that 3D printing brings to measurement and sensor production, paving the way for groundbreaking advancements.

# **KEYWORDS**

 $Auxetic\ structure,\ measurement\ accuracy,\ displacement\ measurement\ method,\ displacement\ sensor,\ 3d\ printing\ technology$ 

## 1. Introduction

Displacement measurements play a pivotal role in various engineering applications, as they are essential for accurately determining the position and motion of objects. The precise determination of displacement holds significant importance across a wide range of engineering disciplines, serving as the fundamental basis for ensuring the integrity, safety, and efficiency of numerous technological processes and systems. Measurement devices typically comprise multiple components, including sensitive elements responsible for detecting the measured variables and conversion elements tasked with transforming the observed variables into electrical signals. These measurement devices can assess various physical properties' changes, such as deformation, strain, and vibration, among others. Displacement measurement equipment plays a pivotal role in engineering and scientific research, providing crucial information about the position and motion of objects.

These displacement measuring devices are designed for versatile applications, ranging from monitoring the structural health of buildings, equipment position control, civil engineering, to various manufacturing sectors (Ming et al., 2022; Reinholz and Seethaler, 2022; Yanlin et al., 2022; Piotr and Piotr, 2022; Shao et al., 2021; Andreas et al., 2020). However, most displacement measurement methods are hindered by the complexity of instrument setup and high costs, inevitably impeding the widespread adoption of displacement sensors. Therefore, considering cost and performance, the design and selection of appropriate measurement devices become particularly crucial. In engineering and scientific research, seeking methods to simplify sensor manufacturing and strategies to reduce the cost of measurement equipment will provide significant

impetus for the application and promotion of displacement measurement. Specifically, if the core components of sensors, such as the sensing elements, can be manufactured through 3D printing, it will result in cost reduction for sensors and significantly broaden the application range of displacement measurement. This progress holds the capacity to transform the realm of displacement measurement by enhancing accessibility and cost-effectiveness for diverse industries and research domains.

In this paper, we introduce a novel approach to measure displacement utilizing a measuring setup comprising an auxetic honeycomb structure, a flat light source, and a solar cell, as illustrated in Figure 1. The proposed method is designed to be simple and easy to implement, making it accessible to a wide range of users. By utilizing the unique properties of the auxetic honeycomb structure, one can measure displacement with acceptable precision. As light shines vertically on the surface of the honeycomb structure, the auxetic structure obstructs a portion of it, allowing the remaining light to pass through and illuminate the surface of the solar cell.

By compressing the auxetic structure, it contracts both longitudinally and laterally, resulting in increased light blocking and a reduction in the output current intensity of the solar cell. This process enables the establishment of a correlation between the displacement change caused by deformation and the intensity of the current. Through this method, we can precisely measure and quantify displacement by analyzing the corresponding changes in the solar cell's output current.

The 3D-printed auxetic honeycomb structure serves as a crucial element in the proposed measurement method. This study thoroughly validates the effectiveness of the proposed approach through rigorous analysis and

Quick Response Code Access this article online



**Website:**Website: www.topicsonchemeng.org.my

DOI:

10.26480/smmp.01.2023.96.101

experimentation. To perform a comparative analysis, the experiments involve the utilization of two distinct auxetic honeycomb structures and one hexagonal honeycomb structure. By systematically comparing the measurement results obtained from these different structures, we can

obtain comprehensive insights into the performance and advantages of our proposed method. This systematic analysis contributes to a better understanding of the capabilities and potential applications of the developed measurement approach.

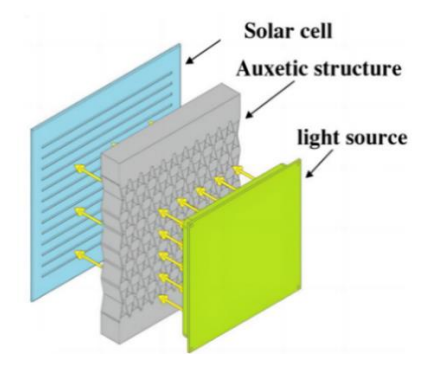


Figure 1: Schematic diagram of proposed method.

# 2. ANALYTICAL AND NUMERICAL MODELS

#### 2.1 Auxetic Structure

Auxetic materials constitute a unique class of substances, distinguished by their remarkable property of lateral expansion when subjected to longitudinal stretching. Owing to these distinctive structural qualities, auxetic materials have found application in various technical fields, such as shock protection, the medical industry, aviation wing design, and even sensor technology (Imbalzano et al., 2017; Lihong et al., 2019; Masoud et al., 2023; A et al., 2022; Budarapu and Natarajan, 2016; J et al., 2023; Frank et al., 2021). Stretchable strain sensors employ mechanical ancillary metamaterials with negative Poisson's ratios because they have a high sensitivity (Taherkhani et al., 2020).

Traditionally, the production of auxetic materials requires intricate mold-making and heat-compression techniques. Nevertheless, advancements in 3D printing technology now enable the creation of auxetic materials and structures with intricate geometries (Al-Furjan et al., 2023).

There are numerous types of honeycomb structures exhibiting negative Poisson's ratio, and this paper specifically adopts two typical auxetic honeycomb structures, both fabricated using 3D printing technology (A et al., 2005; Jackman et al., 1998; Kelkar et al., 2020).

#### 2.2 Theoretical Model of Re-entrant Structure

Figure 2 depicts the visualization of the specimen and illustrates the geometry of the re-entrant structure utilized in this paper.

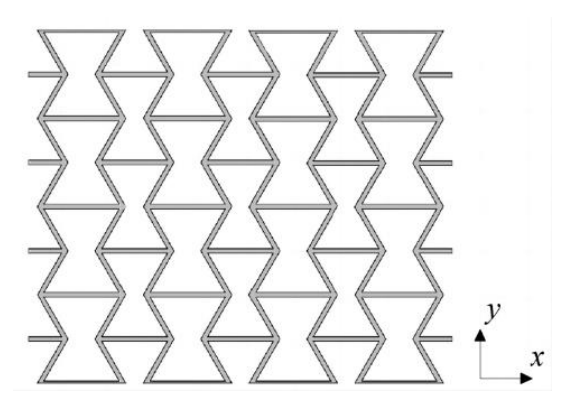


**Figure 2:** Layout of the unit cell (re-entrant structure).

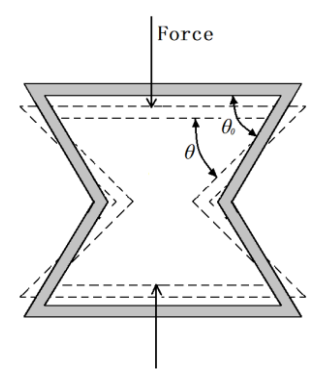


Figure 3: Auxetic effect of the unit cell.

In Figure 3, the overall layout of the re-entrant honeycomb structure is depicted. When the structure is subjected to compression,  $\theta$  will decrease (as illustrated in Figure 3), resulting in a contraction in two dimensions.

The Poisson's ratio of Re-entrant auxetic honeycomb structure is defined as (Vogiatzis et al., 2017):

$$v_{xy} = -\frac{\varepsilon_y}{\varepsilon_x} = \frac{\cos\theta_0 - \frac{h}{l}}{\tan\theta \sin\theta_0} \tag{1}$$

# ${\bf 2.3} \quad \textbf{Theoretical Modal of Circular Element and Ligaments Structure}$

The auxetic structure, as illustrated in Figure 4, comprises circular nodes

with identical radii interconnected by ligaments of equal lengths.

As depicted in Figure 5, the structure exhibits simultaneous vertical contraction and horizontal contraction when compressed, while vertical extension leads to horizontal expansion (Zhang et al., 2013).

# 3. EXPERIMENT

### 3.1 Specimen Geometry

Figure 6 shows printed specimen of re-entrant honeycomb structure (Pattern A) and Figure 7 shows the geometry of the re-entrant structure employed in this paper ( $\theta$ =60°, l=6mm, h=10mm and d=0.5mm).

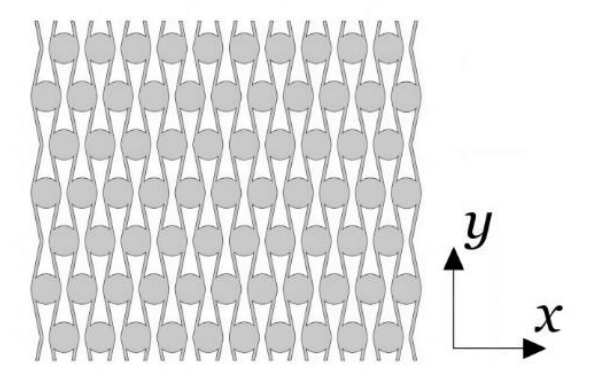
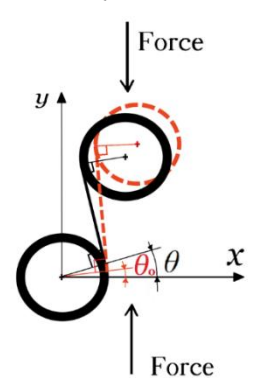


Figure 4: Layout of the unit cell (circular element and ligaments structure).



**Figure 5:** The structure deforms when it is compressed vertically.



 $\textbf{Figure 6:} Specimen of re-entrant\ hexagonal\ honeycomb\ structure.$ 

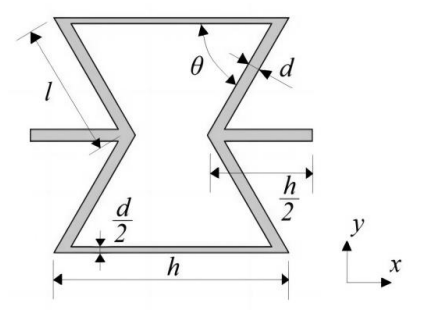


Figure 7: The geometry of the re-entrant structure



Figure 8: Specimen of Circular elements and ligaments honeycomb structure

Figure 8 shows printed specimen of Circular elements and ligaments honeycomb structure (Pattern B).

The external diameter of the circular elements D, the center distance between two adjacent circular elements in the x direction W1 and the center distance between two adjacent circular elements in the y directions W2, the thickness of the straight ligaments h, the length of the straight

ligaments l, and the angle of the straight ligament's perpendicular line to the x axis  $\theta$  are the characteristics of the circular elements and ligaments honeycomb structure.

Figure 9 shows the geometry of the circular elements and ligaments honeycomb structure employed in this paper (W1=3mm, W2=8mm, D=5mm, l=5.8mm, h=0.5mm and  $\theta$ =20°).

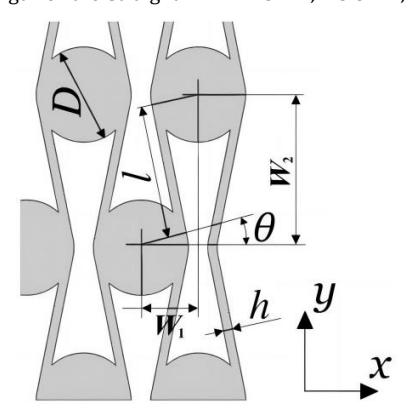


Figure 9: The geometric parameters of the structure

In this paper, we utilized a hexagonal honeycomb structure specimen (Pattern C) as a comparison sample to better demonstrate the function of the auxetic structure in our measurement methodology. Through a comprehensive comparison between the behavior of the auxetic honeycomb structure and the hexagonal honeycomb structure, we successfully showcased the distinctive properties of the auxetic structure and elucidated how these properties significantly contribute to our measurement method. Through this rigorous comparison, we were able to

elucidate the notable advantages of employing an auxetic structure in displacement measurement, thereby offering a more comprehensive understanding of the fundamental principles underpinning our approach. Through conducting this meticulous comparison, we successfully validated the efficacy of our method and acquired valuable insights into potential avenues for further improvement and optimization. As illustrated in Figure 10, the sides of the hexagonal honeycomb structure are represented by l, while the thickness of its cell walls is represented by h.

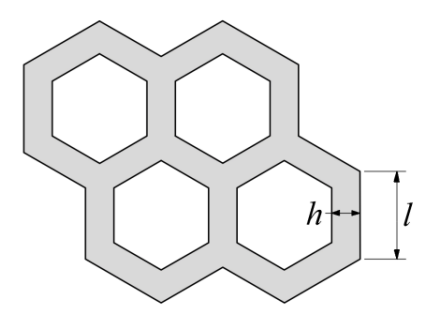


Figure 10: Structure of the hexagon honeycomb structure

Every hexagonal cell has six equal-length edges, and every corner angle is 120 degrees. In this work, the thickness of cell wall is 0.5 mm and l=6mm is used to create Pattern C (Figure 11).

#### 3.2 Specimen Preparation

The specimens were produced utilizing a 3D-SLA printer (utilizing a photosensitive polymer resin that solidifies when exposed to ultraviolet light). The Flexural modulus of the material is 2.2GPa, the Tensile modulus of the material is 2.8GPa and the Poisson's ratio is 0.4.

#### 3.1 Experimental Set-up

The experiments were conducted utilizing a universal testing machine, and the entire procedure was carried out within a darkroom environment to

mitigate the influence of ambient lighting. For the experiment, a plane light source with a luminous surface area of 40×40 mm and an intensity of 360 Lux was employed as the light source.

To measure the solar cell's output voltage, a tunable resistor is connected in series with it. Variations in the incident light on the solar cell result in changes in the generated current intensity, leading to voltage alterations at the two ends of the resistor. A schematic of the experimental setup is illustrated in Figure 12.

The experiment employed a universal testing machine to precisely control the displacement, with compressive loads being applied to the top face of a top plate (refer to Figure 13). The universal testing machine applied a downward force on the specimen, causing it to move precisely 0.1mm with each compression, repeated a total of 10 times.



Figure 11: Hexagon honeycomb structure

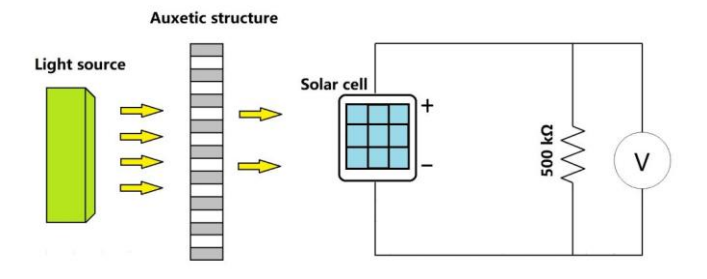


Figure 12: Schematic diagram of the experimental set-up.

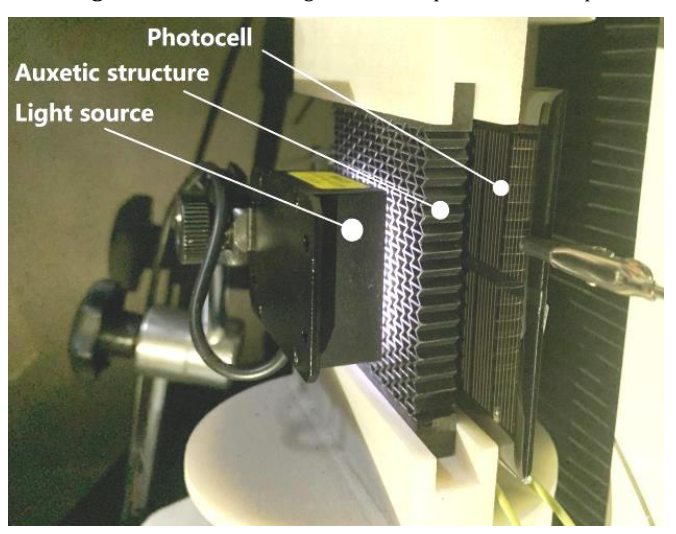


Figure 13: Auxetic structure sample mounted on the test machine.

#### 4. RESULTS AND DISCUSSION

If the specimen is compressed, it will contract in either direction, blocking more light per unit area while also reducing the solar cell's output current. This causes the output voltage  $V_{output}$  to be reduced. The output voltage's initial-state value is designated as V0, and the voltage difference between  $V_{output}$  and  $V_{0}$  is designated as  $\Delta V$ .

$$\Delta V = |V_{output} - V_0| \tag{2}$$

Figure 14 illustrates the correlation between displacement and voltage, acquired through the proposed measurement technique using three distinct honeycomb structures. The scatter plot of diverse data points is depicted in the same figure, and a best-fit line employing the Least Square

Method is incorporated to provide a clearer illustration of the relationship. The slope of the best-fit line serves as a quantification of the sensitivity exhibited by the proposed measurement method.

The rate of slope for the best-fit lines of Patterns A and B, which represent two auxetic honeycomb structures, is observed to be higher than that of the non-auxetic structure Pattern C, as illustrated in Figure 14. Specifically, the slope rate of the line of best fit of Pattern A is 0.015 V/mm, and the slope rate of the line of best fit of Pattern B is 0.013 V/mm, while the slope rate of the line of best fit of Pattern C is 0.011 V/mm. This observation indicates that Patterns A and B demonstrate higher sensitivity compared to Pattern C. This significant finding serves to validate the fundamental concept behind the study.

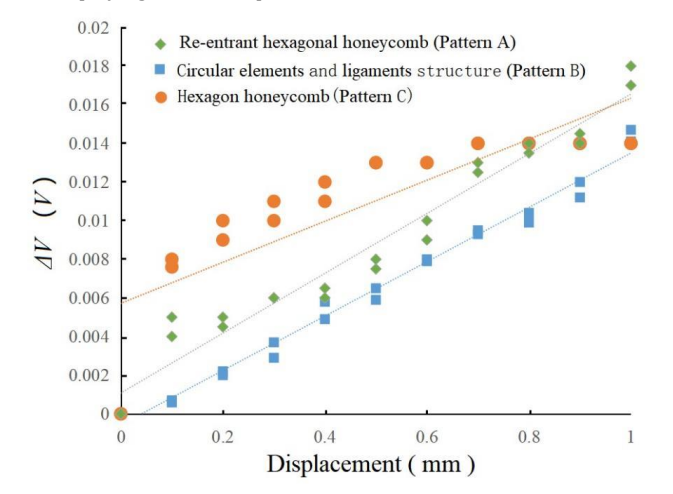


**Figure 14:**  $\Delta V$  -displacement curves.

Like sensitivity, nonlinearity error constitutes a crucial performance indicator for measuring equipment. The displacement-voltage curve of the measurement method utilized in this study, specifically Pattern B, incorporating round components and ligaments honeycomb structures, exhibits a distinct linear behavior for almost the entire range of displacements, up to the point of maximum displacement. Maximum nonlinearity error of the Pattern A is 7.3%, Maximum nonlinearity error of the Pattern C is 32.1%.

Based on the test results, it is evident that the two measurement schemes utilizing negative Poisson's ratio structures demonstrate notable performance advantages when compared to the measurement scheme employing a honeycomb hexagonal structure. The former exhibits enhanced sensitivity and linearity, signifying their superior characteristics.

Through a meticulous comparison of the test results obtained from two distinct measurement schemes utilizing different auxetic structures, it is observed that their sensitivities are comparable. However, Pattern B

exhibits a smaller nonlinearity error when compared to the other measurement scheme.

#### 5. CONCLUSION

This paper introduces a straightforward approach to establish a robust correlation between displacement and electrical signals by utilizing a honeycomb structure as the fundamental component of the proposed measurement method. This method leverages the advantages of 3D printing technology to achieve a straightforward and efficient measurement scheme. Through conducting comparative experiments on three different honeycomb structures, it has been demonstrated that the measurement method employing the irregular structure exhibits superior sensitivity and linearity compared to the method utilizing the hexagonal honeycomb structure. The findings from these experiments provide strong evidence of the enhanced performance achieved through the adoption of the irregular structure, highlighting its potential for precise and reliable displacement measurement. Through comprehensive comparative experiments on three different honeycomb structures, we have thoroughly validated that the measurement method employing the irregular structure demonstrates significantly superior performance in terms of sensitivity and linearity when compared to the method utilizing the hexagonal honeycomb structure. Moreover, harnessing the advantages of 3D printing technology, we have successfully implemented a simple and efficient measurement scheme, effectively reduced processing complexity and production costs while significantly expanding the method's applicability. These findings provide robust scientific support for the feasibility and superiority of our proposed measurement method, while also offering valuable guidance and insights for the future development of sensors and measurement techniques in the field.

#### ACKNOWLEDGEMENT

This work was funded by Xi'an Science and Technology Plan Project, grant number No.2021JH-QCY7-0024

#### REFERENCES

- A. S., M. R., F. S., 2005. Chiral hexagonal cellular sandwich structures: dynamic response. Smart Structures and Materials: Smart Structures and Integrated Systems, 5764, Pp. 695-709. doi:10.1117/12.600021.
- A. V.L., S.F S., A. A.V., 2022. Auxetic Metamaterials for Biomedical Devices: Current Situation, Main Challenges, and Research Trends. Materials, 15 (4), Pp. 1-28. doi:10.3390/MA15041439.
- Al-Furjan, M., Fan, S., Shan, L., Farrokhian, Shen, X., Kolahchi, R., 2023. Wave propagation analysis of micro air vehicle wings with honeycomb core covered by porous FGM and nanocomposite magneto strictive layers. Int. J. Aerosp. doi:10.1080/17455030.2022.2164378
- Andreas, T., Dirk, S., Andreas, F., 2020. In-process workpiece displacement measurements under the rough environments of manufacturing technology. Procedia CIRP, 87, Pp. 409-414. doi: 10.1016/j.procir.2020.02.080.
- Budarapu, R., Natarajan, R., 2016. Design concepts of an aircraft wing: composite and morphing airfoil with auxetic structures. Frontiers of structural and civil engineering, 10 (4), Pp. 394-408. doi:10.1007/s11709-016-0352-z.
- Frank, C., Mark, M., Forian, B., 2021. 2D Printing of Piezoresistive Auxetic Silicone Sensor Structures. Ieee Robotics And Automation Letters, 6 (2), Pp. 2541-2546. doi:10.1109/LRA.2021.3062000.

- Imbalzano, G., Linforth, S., Ngo, D.T., 2017. Blast resistance of auxetic and honeycomb sandwich panels: Comparisons and parametric designs. Composite Structures, 183, Pp. 242-261. doi: 10.1016/j.compstruct.2017.03.018.
- J. TC., C. B.H., Pierre, R., 2023. HACS: Helical Auxetic Yarn Capacitive Strain Sensors with Sensitivity Beyond the Theoretical Limit (Adv. Mater. 10/2023). Advanced Materials, 35 (10). doi:10.1002/ADMA.202370072.
- Jackman, J.R., Brittain, T.S., Adams, A., 1998. Design and Fabrication of Topologically Complex, Three – Dimensional Microstructures. Science, 280 (5372), Pp. 2089-2091. doi:10.1126/science.280.5372.2089.
- Kelkar, U.P., Kim, S.H., Cho, K., 2020. Cellular Auxetic Structures for Mechanical Metamaterials: A Review. Sensors, 20 (11), Pp. 31-32. doi:10.3390/s20113132.
- Lihong, Y., Lei, S., Xuyang, L., 2019. Sandwich plates with gradient lattice cores subjected to air blast loadings. Mechanics of Advanced Materials and Structures, 28 (13), Pp. 1355-1366. doi:10.1080/15376494.2019.1669092.
- Masoud, S., Ali, Z., Mahdi, B., 2023. Auxetic metamaterials for bone-implanted medical devices: Recent advances and new perspectives. European Journal of Mechanics A Solids, Pp. 98. doi: 10.1016/J.EUROMECHSOL.2022.104905.
- Ming Z.W., Lin, G., Zailin, Y., 2022. Overall structural seismic damage rapid assessment method based on period and displacement response characteristics. Scientific Reports, 12 (1), Pp. 19-22. doi: 10.1038/S41598-022-23927-X.
- Piotr, S., Piotr, K., 2022. Effectiveness of Selected Strain and Displacement Measurement Techniques in Civil Engineering. Buildings, 12 (2), Pp. 172. doi:10.3390/BUILDINGS12020172.
- Reinholz, B.A., Seethaler, R.J., 2022. Sensor Fusion of Self-Sensed Measurements for Position Control of a Constant Air-Gap Solenoid. IEEE sensors journal, 22 (24), Pp. 23997-24005. doi:10.1109/JSEN.2022.3216311.
- Shao, Y.D., Li, L., Li, J., An, S.J., Hao, H., 2021. Computer vision-based targetfree 3D vibration displacement measurement of structures. Engineering Structures, 246, Pp. 113040. doi: 10.1016/j.engstruct.2021.113040
- Taherkhani, B., Azizkhani, B.M., Kadkhodapour, J., 2020. Highly sensitive, piezoresistive, silicone/carbon fiber-based auxetic sensor for low strain values. Sensors and Actuators: A. Physical, 305, Pp. 111939. doi: 10.1016/j.sna.2020.111939.
- Vogiatzis, P., Chen, S., Wang, X., Li, T., and Wang, L., 2017. Study of an auxetic structure made of tubes and corrugated sheets. Computer-Aided Design., 83, Pp. 15-32. doi: 10.1016/j.cad.2016.09.009
- Yanlin, L., Benke, Q., Linqing, Y., 2022. Static calibration experiments of capacitance control rod position Measurement sensor. Progress in Nuclear Energy, 152, Pp. 104370. doi: 10.1016/J.PUNCENE.2022.104370
- Zhang, Z., Hu, H., Liu, S., 2013. Study of an auxetic structure made of tubes and corrugated sheets. Physical status solidi (b), 250 (10), Pp. 1996-2001. doi:10.1002/pssb.201248349.

